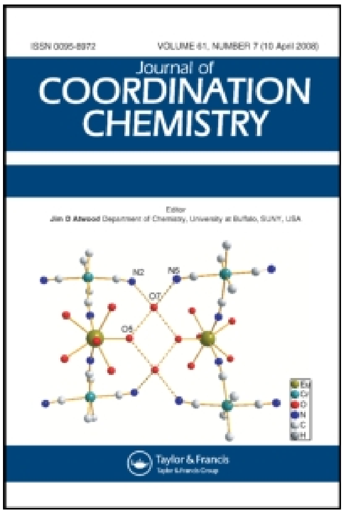

Journal of Coordination Chemistry
Publication details, including instructions for authors and subscription information:
http://www.informaworld.com/smpp/title~content=t713455674

Synthesis, Spectral and Magnetic Studies of Mononuclear and Binuclear Mn(Ii), Co(Ii), Ni(Ii) and Cu(Ii) Complexes with Semicarbazone Ligands Derived from Sulfonamide

A. A. Saleh[a]; S. M. E. Khalil[a]; M. F. Eid[a]; M. A. El-Ghamry[a]
[a] Department of Chemistry, Faculty of Education, Ain Shams University, Cairo, Egypt

To cite this Article Saleh, A. A. , Khalil, S. M. E. , Eid, M. F. and El-Ghamry, M. A.(2003) 'Synthesis, Spectral and Magnetic Studies of Mononuclear and Binuclear Mn(Ii), Co(Ii), Ni(Ii) and Cu(Ii) Complexes with Semicarbazone Ligands Derived from Sulfonamide', Journal of Coordination Chemistry, 56: 6, 467 — 480

To link to this Article: DOI: 10.1080/0095897031000099992

URL: http://dx.doi.org/10.1080/0095897031000099992

J. Coord. Chem., 2003, Vol. 56, No. 6, pp. 467–480

Taylor & Francis
Taylor & Francis Group

SYNTHESIS, SPECTRAL AND MAGNETIC STUDIES OF MONONUCLEAR AND BINUCLEAR Mn(II), Co(II), Ni(II) AND Cu(II) COMPLEXES WITH SEMICARBAZONE LIGANDS DERIVED FROM SULFONAMIDE

A.A. SALEH*, S.M.E. KHALIL, M.F. EID and M.A. EL-GHAMRY

Department of Chemistry, Faculty of Education, Ain Shams University, Cairo, Egypt

(Received 22 Feburary 2002; Revised 8 July 2002; In final form 8 January 2003)

Mononuclear and binuclear Mn(II), Co(II), Ni(II) and Cu(II) complexes of new semicarbazone ligands derived from sulfonamide were synthesized and characterized by elemental analysis and IR spectra. In mononuclear complexes, the semicarbazone behaves as a monoanionic terdentate or neutral terdentate ligand towards the metal ion. However, in binuclear complexes, it behaves as a monoanionic terdentate towards one of the bivalent metal ions and monoanionic bidentate ligand towards the other metal ion in the same complex. Electronic spectra and magnetic susceptibility measurements of the solid complexes indicated octahedral geometry around Mn(II), Co(II) and Ni(II) and square planar around the Cu(II) ion. These geometries were confirmed by the results obtained from thermal analyses. The antifungus properties of the ligands and their complexes were investigated.

Keywords: Semicarbazone complexes; Mono- and binuclear-transition metal complexes

INTRODUCTION

Semicarbazone derivatives of various transition metals have been investigated owing to their coordinating capability and pharmaceutical activities [1–5]. We report the synthesis, structures and properties of a series of new complexes with some N^4-(aryl) semicarbazones derived from sulfonamide.

EXPERIMENTAL

The chemicals used were BDH products. The solvents used were purified by recommended procedures [6]. The apparatus, physical measurements and analyses are the same as previously described [7,8].

---

*Corresponding author. E-mail: tcsran@soficom.com.eg

ISSN 0095-8972 print: ISSN 1029-0389 online
DOI: 10.1080/0095897031000099992

Preparation of Ethyl Carboxyaniline-4 Sulfonamide

Ethyl chloroformate (1.08 g, 0.01 mol) was added dropwise to sulfanilamide (1.72 g, 0.01 mol) in DMF (50 mL). The reaction mixture was refluxed on a hot plate for 1 h. The product was allowed to cool to room temperature, filtered off and recrystallized from ethanol to give reddish white crystals, m.p. 213°C.

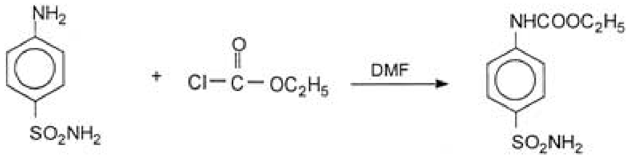

Preparation of Semicarbazide-4yl-Benzene Sulfonamide (SBS)

The hydrazine hydrate (99%) (1 g, 0.02 mol) was added dropwise to ethyl carboxyaniline-4 sulfonamide (2.44 g, 0.01 mol) in DMF (50 mL). The reaction mixture was refluxed on a hot plate for about 4 h, then cooled. The solid product was filtered off and recrystallized from ethanol to give light white crystals, m.p. 221°C.

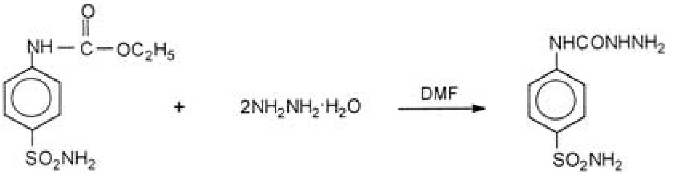

Preparation of Semicarbazone Ligands, SSBS, SSBSS, HASBS and NBSBS

A mixture of (2.30 g, 0.01 mol) semicarbazide-4yl-benzene sulfonamide (SBS) and (1.22 g, 0.01 mol) salicylaldehyde or (1.36 g, 0.01 mol) *o*-hydroxyacetophenone in 50 mL DMF was refluxed for 1 h. In the case of *o*-nitrobenzaldehyde (1.52 g, 0.01 mol), the mixture was refluxed for 15 h. The reaction with salicylaldehyde (2.44 g, 0.02 mol) was repeated at a longer reflux time, 15 h. The reaction mixture was concentrated and cooled. The solid products were filtered off and recrystallized from ethanol. The following scheme shows the preparation of substituted semicarbazones-4yl-benzene salfonamide.

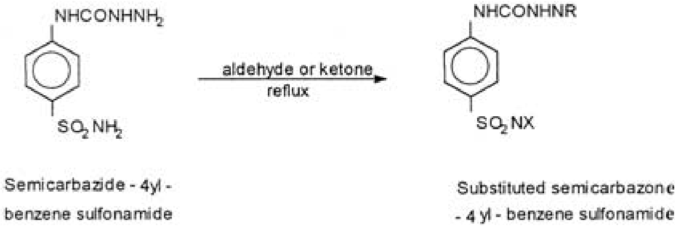

Compound	*X*	*R*	*Time of reflux* (h)	*m.p.* (°C)
SSBS (L^1)	H_2	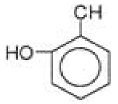	1	231
SSBSS (L^2)	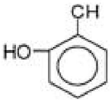	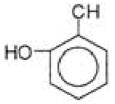	15	193
HASBS (L^3)	H_2	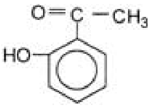	1	234
NBSBS (L^4)	H_2	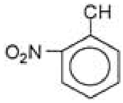	15	171

SSBS = salicylaldehyde semicarbazone-4yl-benzene sulfonamide.
SSBSS = salicylaldehyde semicarbazone-4yl-benzene salicylaldehyde sulfonamide.
HASBS = 2-hydroxyacetophenone semicarbazone-4yl-benzene sulfonamide.
NBSBS = 2-nitrobenzaldehyde semicarbazone-4yl-benzene sulfonamide.

The purity of the ligand was examined by elemental analysis, IR, ^{1}H NMR and mass spectra. Anal. Calcd L^1: C, 50.30; H, 4.19; N, 16.70; S, 9.58. Found: C, 49.50; H, 3.70; N, 17.00; S, 9.50, Calcd L^2: C, 57.53; H, 4.20; N, 12.78; S, 7.30. Found: C, 57.10; H, 4.60; N, 13.00; S, 6.90, Calcd L^3: C, 48.24; H, 5.53; N, 14.07; S, 8.04. Found: C, 48.30; H, 5.70; N, 14.30; S, 8.40, Calcd L^4: C, 44.10; H, 3.94; N, 18.37; S, 8.40. Found: C, 44.80; H, 4.10; N, 18.10; S, 8.20. The colors of the ligands L^1, L^2, L^3 and L^4 were yellow, yellowish brown, yellowish white and yellowish brown, respectively. IR (cm^{-1}), ν_{as} NH 3295–3346, ν_s NH 3225–3300 cm^{-1} of NH$_2$, νOH...N, 3040–3150 cm^{-1}, νC=O, 1690–1715 cm^{-1}; νC=N, 1555–1600 cm^{-1} and νCONH, 1505–1530 cm^{-1}. For $L^1 - L^4$, ν_3SO_2 1150–1160, ν_1SO_2 1050–1060 and ν_4SO_2 385–395 cm^{-1}. Resonance between the ketonic and enolic forms of each of these ligands is shown in the following scheme:

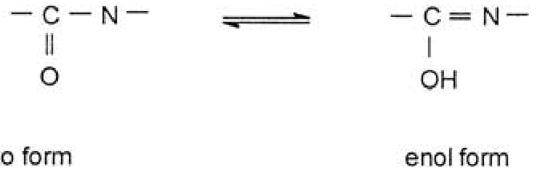

$$-\underset{\underset{O}{\|}}{C}-N- \rightleftharpoons -\underset{\underset{OH}{|}}{C}=N-$$

^{1}H NMR, δ(ppm), δOH phenolic 9.00–9.75, δCH=N 8.30–8.90, δCH aromatic 6.90–7.60 and δNH 3.15–3.30. The mass spectra of each compound corresponded to its molecular weight (*m*/*e*).

Synthesis of New Mn(II), Co(II), Ni(II) and Cu(II) Semicarbazone Complexes

2 mmole of LiOH dissolved in the minimum of twice distilled water (~2 mL) was added to 1 mmol of the ligand dissolved in 50 mL of ethanol to convert it to the ionic form. The mixture was stirred for 30 min, then 1 mmol of the metal salt, $MnCl_2 \cdot 4H_2O$, $Co(NO_3)_2 \cdot 6H_2O$, $NiCl_2 \cdot 6H_2O$ or $CuSO_4 \cdot 5H_2O$ dissolved in distilled water (~5 mL) was added to the mixture. The reaction mixture was stirred for 5 h during which the solid complex precipitated. It was then filtered off, washed several times with distilled water, then a small amount of ethanol to remove any traces of the metal ions or free ligands, and finally washed with diethyl ether and then dried *in vacuo*.

RESULTS AND DISCUSSION

Elemental analyses of the prepared Mn(II), Co(II), Ni(II) and Cu(II) complexes with semicarbazone derivatives (Table I) indicate that the stoichiometries are either (1 : 1) (M : L), denoting the formation of mononuclear complexes of L^1, L^3 and L^4 in which the semicarbazone ligand L^1 and L^3 behave as monoanionic terdentate and L^4 behaves as neutral terdentate ligand towards the divalent metal ion or (2 : 1) (M : L), denoting the formation of binuclear complexes of the ligand L^2 in which the semicarbazone ligand behaves as a monoanionic terdentate ligand toward one of the divalent metal ions and as a monoanionic bidentate ligand toward the other metal ion in the same complex.

Thermogravimetric Analysis

Thermogravimetric analysis (TGA) (Table II) of some solid complexes indicate that they exhibit common behavior. The thermograms can be subdivided into five main regions: the first region extends up to 125°C representing the removal of lattice water or ethanol molecules. The second region extending up to 310°C includes the elimination of water or ethanol molecules involved in coordination with the central metal (II) ion. The third region extending up to 380°C includes the elimination of noncoordinated or coordinated Cl^- or NO_3^- or SO_4^{-2} ions. In the fourth region, thermal stability extends up to 535°C. The fifth region extending up to 800°C represents decomposition of the complex through removal of the ligand leading to the metal oxide. The metal content in the residue was calculated and found to be consistent with the results of the elemental analysis of the complexes.

Spectral Measurements

The IR spectra of the Mn(II), Co(II), Ni(II) and Cu(II) complexes compared to the free ligands (Table III) indicates the following: (1) The IR spectra of all complexes exhibit a broad band around (3420–3543) cm^{-1} which is attributed to a νOH of a water and/or ethanol molecule associated with the complex formation. (2) The ligands L^1, L^3 and L^4 display bands at (3305–3320) and (3220–3230) cm^{-1} assignable to ν_{as} and ν_s of NH_2, respectively. These bands remain almost intact in the spectra of the mononuclear complexes showing their nonparticipation in the chelation. (3) The ligands L^1, L^2 and L^3 show a broad band at 3040–3110 cm^{-1} due to the phenolic OH group of the conjugate

TABLE I Elemental analysis and some physical properties of the solid complexes of L^1, L^2, L^3 and L^4

Complex	*M : L*	*Color*	*m.p.* (°C)	*F. W*	*Analysis Found % (Calculated %)*				
					%C	*%H*	*%N*	*%S*	*%M*
$[MnL^1(H_2O)_3]Cl \cdot 3H_2O$	1 : 1	Gray	318	531.4	31.5 (31.6)	4.2 (4.7)	10.2 (10.5)	6.2 (6.0)	10.7 (10.3)
$[CoL^1(H_2O)_3]NO_3 \cdot 5H_2O$	1 : 1	Brown	260	597.8	27.7 (28.1)	4.8 (4.8)	11.5 (11.7)	5.2 (5.4)	9.6 (9.9)
$[NiL^1(H_2O)_3]Cl \cdot 2H_2O \cdot EtOH$	1 : 1	Light green	> 350	563.2	34.6 (34.1)	4.5 (5.1)	10.0 (9.9)	5.6 (5.7)	10.2 (10.4)
$[CuL^1(H_2O)_3]_2SO_4 \cdot 2H_2O \cdot EtOH$	1 : 1	Dark green	242	1079.0	33.5 (33.4)	4.5 (4.5)	10.3 (10.4)	8.8 (8.9)	11.9 (11.8)
$[Mn_2L^2Cl_2(H_2O)_5] \cdot 6H_2O$	2 : 1	Gray	250	814.86	30.8 (31.0)	4.4 (4.7)	6.7 (6.9)	3.8 (3.9)	13.9 (13.5)
$[Co_2L^2(NO_3)(H_2O)_6]$	2 : 1	Olive green	> 350	722.86	35.1 (34.9)	3.8 (3.7)	9.5 (9.7)	4.5 (4.4)	16.7 (16.3)
$[Ni_2L^2(Cl)_2(H_2O)_5]$	2 : 1	Green	298	714.40	35.2 (35.3)	3.9 (3.6)	7.7 (7.8)	4.4 (4.5)	16.0 (16.4)
$[Cu_2L^2(H_2O)_3]_2SO_4 \cdot H_2O$	2 : 1	Brown	302	1346.0	36.9 (37.4)	2.7 (3.3)	8.2 (8.3)	7.2 (7.1)	18.4 (18.9)
$[MnL^3(H_2O)_3]Cl \cdot H_2O$	1 : 1	Brown	240	509.4	35.6 (35.3)	4.0 (4.5)	10.8 (11.0)	6.4 (6.3)	11.2 (10.8)
$[CoL^3(H_2O)_3]NO_3 \cdot EtOH$	1 : 1	Olive green	287	567.9	35.4 (35.9)	4.2 (4.8)	12.4 (12.3)	5.5 (5.6)	10.7 (10.4)
$[NiL^3(H_2O)_3]Cl \cdot 4H_2O$	1 : 1	Green	310	567.2	31.3 (31.7)	4.8 (5.1)	9.7 (9.9)	5.7 (5.6)	10.6 (10.4)
$[CuL^3(H_2O)_2(EtOH)]_2SO_4$	1 : 1	Dark brown	238	1081	37.2 (37.7)	4.0 (4.6)	10.5 (10.4)	8.8 (8.9)	12.2 (11.8)
$[MnL^4(H_2O)_3Cl_2 \cdot 3H_2O$	1 : 1	Drak brown	237	596.9	28.5 (28.1)	4.5 (4.2)	11.6 (11.7)	5.4 (5.4)	9.5 (9.2)
$[CoL^4_2] \cdot 2EtOH$	1 : 2	Brown	231	874.9	44.3 (43.8)	4.2 (4.1)	16.1 (16.0)	7.2 (7.3)	7.1 (6.7)
$[NiL^4(EtOH)_2H_2O]Cl_2 \cdot H_2O$	1 : 1	Green	> 350	588.7	36.5 (36.7)	4.8 (4.9)	11.8 (11.9)	5.6 (5.4)	9.6 (10.0)
$[CuL^4(H_2O)_3]SO_4 \cdot 2H_2O$	1 : 1	Dark brown	249	612.5	27.9 (27.4)	4.2 (3.7)	11.3 (11.4)	10.7 (10.5)	10.3 (10.4)

TABLE II Thermogravimetric analysis of Mn(II), Co(II), Ni(II) and Cu(II) complexes

Complex	*Temp. range* (°C)	*% Loss calc. (found)*	*Lost fragments*	*Residue*
$[MnL^1(H_2O)_3]Cl \cdot 3H_2O$	50–125	10.2 (10.3)	3 H_2O lattice	$[Mn\ L^1(H_2O)_3]Cl$
	125–240	10.2 (10.3)	3 H_2O coordinated	$[Mn\ L^1]Cl$
	240–270	6.7 (6.6)	Loss of Cl^- ion	$[Mn\ L^1]$
	365–535		Thermal stability	
	535–800	62.7 (62.5)		MnO
$[Mn_2L^2Cl_2(H_2O)_5] \cdot 6H_2O$	30–110	13.2 (12.9)	6 H_2O lattice	$[Mn_2\ L^2Cl_2(H_2O)_5]$
	120–200	11.0 (11.1)	5 H_2O coordinated	$[Mn_2\ L^2Cl_2]$
	230–380	8.7 (8.9)	2 Cl^- ion coordinated	$[Mn_2\ L^2]$
	455–480		Thermal stability	
	550–700	53.5 (53.1)		2 MnO
$[MnL^3(H_2O)_3]Cl \cdot H_2O$	30–55	3.5 (3.7)	One H_2O lattice	$[Mn\ L^3(H_2O)_3]Cl$
	107–225	10.6 (11.1)	3 H_2O coordinated	$[Mn\ L^3]Cl$
	225–304	6.9 (6.5)	Loss of a Cl^- ion	$[Mn\ L^3]$
	430–475		Thermal stability	
	475–725	68.1 (67.9)		MnO
$[MnL^4(H_2O)_3Cl_2 \cdot 3H_2O$	19.6–70.2	9.0 (9.1)	3 H_2O lattice	$[Mn\ L^4(H_2O)_3]Cl_2$
	120–230	9.0 (9.1)	3 H_2O coordinated	$[Mn\ L^4]2Cl$
	230–265	11.9 (11.6)	2 Cl^- ion coordinated	$[Mn\ L^4]$
	420–440		Thermal stability	
	440–880	68.1 (67.9)		MnO
$[CoL^1(H_2O)_3]NO_3 \cdot 5H_2O$	34–250	24.0 (24.1)	$5H_2O$ lattice	$[Co\ L^1(H_2O)_3]NO_3$
			and $3H_2O$ coordinated	$[Co\ L^1]NO_3$
	284–313	10.4 (10.5)	Loss of a $NO_3{}^-$ ion	$[Co\ L^1]$
	450–480		Thermal stability	
	520–690	55.7 (55.5)		CoO
$[Co_2L^2(NO_3)(H_2O)_6]$	144–250	14.9 (15.0)	6 H_2O coordinated	$[Co_2\ L^2(NO_3)]$
	250–296	8.6 (8.6)	Loss of a	$[Co_2\ L^2]$
			coordinated $NO_3{}^-$	
	296–310		Thermal stability	
	410–789	60.2 (59.9)		2CoO
$[CoL^3(H_2O)_3]NO_3 \cdot EtOH$	22.9–80.1	8.1 (8.6)	One EtOH lattice	$[Co\ L^3(H_2O)_3]NO_3$
	110–250	9.5 (9.5)	3 H_2O coordinated	$[Co\ L^3]NO_3$
	250–273	10.9 (10.9)	Loss of a $NO_3{}^-$ ion	$[Co\ L^3]$
	470–490		Thermal stability	
	490–671	61.1 (60.6)		CoO
$[CoL^4_2] \cdot 2EtOH$	26.1–85.0	10.8 (10.9)	2 EtOH lattice	$[Co\ L_2{}^4]$
	180–220		Thermal stability	
	326–700	82.18 (82.11)		CoO
$[NiL^1(H_2O)_3]Cl \cdot 2H_2O \cdot EtOH$	21–93	8.2 (8.3)	EtOH lattice one	$[Ni\ L^1(H_2O)_3]Cl \cdot 2H_2O$
	93–223	15.9 (16.1)	2 H_2O lattice and	$[Ni\ L^1(H_2O)_3]Cl$
			3 H_2O coordinated	$[NiL^1]Cl$
			Loss of a Cl^- ion	$[NiL^1]$
	223–243	6.3 (6.3)		
	250–260		Thermal stability	NiO
	475–600	59.13 (58.8)		
$[Ni_2L^2(Cl)_2(H_2O)_5]$	110–279	12.6 (12.6)	5 H_2O coordinated	$[Ni_2\ L^2Cl_2]$
	279–300	9.9 (9.9)	Cl^- ion coordinated	$[Ni_2\ L^2]$
	450–480		Thermal stability	
	500–639	61.0 (60.9)		NiO
$[NiL^3(H_2O)_5]Cl \cdot 4H_2O$	50–300	22.21 (21.90)	2 H_2O lattice and	$[Ni\ L^3(H_2O)_3]Cl$
			3 H_2O coordinated	$[Ni\ L^3]Cl$
	300–320	6.26 (6.25)	Loss of a Cl^- ion	$[Ni\ L^3]$
	320–330		Thermal stability	
	330–688	61.18 (61.54)		[NiO]

(*Continued*)

TABLE II Continued

Complex	*Temp. range* (°C)	*% Loss calc. (found)*	*Lost fragments*	*Residue*
$[NiL^4(EtOH)_2H_2O]Cl_2 \cdot H_2O$	34–80	3.06 (3.00)		$[NiL^4(EtOH)_2H_2O]Cl_2$
	110–289	18.69 (18.50)	2 EtOH coordinated	$[NiL^4H_2O]Cl_2$
			and one H_2O coordinated	$[NiL^4]Cl_2$
			Loss 2 Cl^- ions	$[NiL^4]$
	289–319	12.06 (12.00)		
	319–340		Thermal stability	
	401–694	56.23 (56.5)		[NiO]
$[CuL^1(H_2O)_3]_2SO_4 \cdot 2H_2O \cdot EtOH$	50–80	4.26 (4.48)	One EtOH lattice	$[CuL^1(H_2O)_3]_2SO_4 \cdot 2H_2O$
	80–260	13.35 (13.48)	2 H_2O lattice and	$[CuL^1(H_2O)_3]_2SO_4$
			3 H_2O coordinated	$[CuL^1]_2SO_4$
	260–274	8.90 (8.99)	Loss of SO_4^{-2} ion	$[CuL^1]_2$
	307–320		Thermal stability	
	361–695	61.72 (61.33)		2 CuO
$[Cu_2L^2(H_2O)_3]_2SO_4 \cdot H_2O$	24.59–94.75	1.34 (1.50)	One H_2O lattice	$[Cu_2L^2(H_2O)_3]_2SO_4$
	135–310	8.02 (8.00)	6 H_2O coordinated	$[Cu_2L^2]_2SO_4$
	310–322	7.13 (7.00)	Loss of a SO_4^{-2} ion	$[Cu_2L^2]_2$
	322–342		Thermal stability	
	342–660	64.62 (64.50)		4 CuO
$[CuL^3(H_2O)_2(EtOH)]_2SO_4$	135–268	15.54 (15.19)	2EtOH coordinated	$[CuL^3(H_2O)_3]_2SO_4$
			and 4 H_2O coordinated	$[CuL^3]_2SO_4$
	277–295	8.88 (8.82)	Loss of a SO_4^{-2} ion	$[CuL^3]_2$
	380–400		Thermal stability	
	450–558	64.19 (64.19)		2 CuO
$[CuL^4(H_2O)_3]SO_4 \cdot 2H_2O$	75–90	5.88 (5.61)	2 H_2O lattice	$[CuL^4(H_2O)_3]SO_4$
	123–153	8.82 (9.18)	3 H_2O coordinated	$[CuL^4]\ SO_4$
	226–279	15.67 (15.31)	Loss of SO_4^{-2} ion	$[CuL^4]$
	279–289		Thermal stability	
	301–673	59.26 (59.69)		CuO

chelate ring involving the OH...N=C hydrogen bond [9]. This band disappears on complex formation indicating the deprotonation of the phenolic OH group and the coordination of the metal ion to the phenolic oxygen atom [10,11]. (4) The νC=O is observed in all ligands around 1700–1715 cm^{-1} and shifts lower by 5–15 cm^{-1} in mononuclear complexes of the L^1, L^3 and L^4 ligands and shifts higher by 10 cm^{-1} in the binuclear complexes of L^2 except the Co(II) and Cu(II) complexes, indicating the bonding of the carbonyl oxygen to the metal ion. In the case of Co(II) and Cu(II) complexes of ligand L^2 this band totally disappears due to keto–enol tautomerism and the deprotonation of the hydrogen atom of the enolic form. (5) The νC=N observed around 1590–1600 cm^{-1} in all ligands shifts by 5–15 cm^{-1} lower in the mononuclear complexes of L^1, L^3 and L^4 ligands and shifts higher by 5–20 cm^{-1} in the binuclear complexes of L^2 ligand. However, the observed decrease in this frequency is not that large because this group is conjugated to a benzene ring [12,13]. (6) The bands due to ν_3SO_2, ν_1SO_2 and ν_2SO_2 are located at 1160, 1060 and 390 cm^{-1}, respectively, in the IR spectra of L^1, L^3 and L^4 ligands and remain at the same position in the IR spectra of the metal complexes, indicating that the SO_2 group does not participate in complex formation. For binuclear complexes of L^2, ν_3SO_2, ν_1SO_2 and ν_2SO_2 located at 1150, 1050 and 385 cm^{-1} in the IR spectra of the ligand L^2, shift ±5–45 cm^{-1} in the complexes indicating the disturbance of the SO_2 group by the formation of the near chelate ring. (7) Two new bands appear in the IR spectra of all metal chelates which are absent in the IR spectra of the free ligands at

TABLE III Important IR spectral bands (cm^{-1}) and their assignment for ligands L^1, L^2, L^3 and L^4 and their metal complexes

Compound	ν_{H_2O}	ν_{asNH_2}	ν_{sNH_2}	ν_{N-H}	$\nu_{OH\cdots N}$	$\nu_{C=O}$	$\nu_{C=N}$	ν_{CON}	ν_{3SO_2}	ν_{1SO_2}	$\delta_{CH_{aromatic}}$	$\delta_{NH_{outofplane}}$	ν_{M-O}	ν_{M-N}	ν_{4SO_2}	*Other bands*
L^1	–	3305	3225	–	3110–3060	1710	1600	1530	1160	1060	715	670	–	–	390	–
[MnL^1(H$_2$O)$_3$]Cl · 3H$_2$O	3480	3300	3220	–	–	1700	1590	1523	1160	1060	710	670	543	425	390	–
[CoL^1(H$_2$O)$_3$]NO$_3$ · 5H$_2$O	3480	3300	3220	–	–	1695	1585	1520	1160	1060	720	650	547	445	390	νNO_3^- 1400
[NiL^1(H$_2$O)$_3$] Cl · 2H$_2$O · EtOH	3543	3302	3224	–	–	1705	1595	1518	1160	1060	715	660	543	440	390	–
[CuL^1(H$_2$O)$_3$]$_2$ SO$_4$ · 2H$_2$O · EtOH	3485	3305	3230	–	–	1700	1588	1525	1160	1060	715	660	547	440	390	νSO_4^{-2} 1160
L^2	–	3290	3220	3290–3220 broad	3040–3100 broad	1700	1590	1520	1150	1050	710	650	–	–	385	–
[Mn$_2$L^{2}Cl$_2$(H$_2$O)$_5$] · 6H$_2$O	3470	–	–	3395–3220 broad	–	1710	1595	1530	1155	1055	710	655	540	435	390	Mn–Cl 340
[Co$_2$L^2(NO$_3$)(H$_2$O)$_6$]	3480	–	–	3340–3240 broad	–	–	1610	–	1150	1095	760	610	560	420	–	M–NO$_3$ $\nu_1$1440 ν_5 1325
[Ni$_2$L^2(Cl)$_2$(H$_2$O)$_5$]	3460	–	–	3320–3220 broad	–	1710	1595	1530	1160	1060	715	660	545	445	388	Ni–Cl 342
[Cu$_2$L^2(H$_2$O)$_3$]$_2$SO$_4$ · H$_2$O	3420	–	–	3400–3215 broad	–	–	1605	–	1150	1090	755	600	555	460	355	$\nu_3 SO_4^{-2}$ 1150
L3	–	3320	3220	–	3115–3060	1710	1595	1535	1160	1060	715	660	–	–	395	–
[Mn L^3(H$_2$O)$_3$]Cl · H$_2$O	3450	3320	3225	–	–	1700	1590	1530	1160	1060	720	660	544	442	395	–
[CoL^3(H$_2$O)$_3$]NO$_3$ · EtOH	3460	3320	3220	–	–	1705	1590	1530	1155	1055	715	660	546	442	395	$\nu_3 NO_3^-$ 1380
[NiL^3(H$_2$O)$_3$]Cl · 4H$_2$O	3440	3320	3220	–	–	1705	1592	1530	1160	1060	715	660	542	440	395	–
[CuL^3(H$_2$O)$_2$(EtOH)]$_2$SO$_4$	3460	3300	3220	–	–	1700	1590	1520	1150	1050	710	655	550	446	395	$\nu_3 SO_4^{-2}$ 1150
L^4	–	3320	3230	–	–	1715	1590	1525	1155	1059	715	660	–	–	390	νNO_2 1400
[MnL^4(H$_2$O)$_3$]Cl$_2$ · 3H$_2$O	3440	3300	3220	–	–	1705	1594	1530	1155	1055	710	650	540	440	388	νNO_2 1405, 1330, δ,825
[CoL$_2$^{4}] · 2EtOH	3460	3310	3220	–	–	1705	1595	1530	1157	1055	710	650	548	450	390	νNO_2 1408, 1330, δ,825
[NiL^4(EtOH)$_2$H$_2$O]Cl$_2$ · H$_2$O	3440	3320	3230	–	–	1700	1598	1530	1157	1060	715	660	548	450	390	νNO_2 1410, 1315, δ,840
[CuL^4(H$_2$O)$_3$]SO$_4$ · 2H$_2$O	3460	3320	3225	–	–	1710	1595	1530	1157	1060	720	655	548	442	390	$\nu_3 SO_4^{-2}$ 1157 νNO_2 1410, 1315, δ,835

(542–560) and (420–460) cm^{-1} which can be assigned to νM–O and νM–N. (8) The C=O originating through resonance between the keto and enol forms of the ligands gives rise to a C=O band observed around (1520–1535) cm^{-1} in the spectra of all ligands and shifted lower by 5–15 cm^{-1} in all complexes except the binuclear complexes of Co^{2+} and Cu^{2+} which did not exhibit the carbonyl stretching band. This is good evidence for enolization of the semicarbazone residue [9]. Also, the Cu^{2+} and Co^{2+} complexes did not show any characteristic frequencies of the amide group (NHCO); instead a new sharp band is observed at 1530 cm^{-1} indicating the presence of $\rangle\mathrm{C{=}N{-}N{=}C}\langle$ [14], which is also evidence for enolization analogous to those of azines. (9) In mononuclear complexes $[\mathrm{CoL}^1(\mathrm{H_2O})_3]\mathrm{NO_3}\cdot 5\mathrm{H_2O}$ and $[\mathrm{CoL}^3(\mathrm{H_2O})_3]\mathrm{NO_3}\cdot \mathrm{EtOH}$, the $\nu_3\mathrm{NO_3}$ is at 1400 and 1380 cm^{-1}, respectively, supporting the uncoordinated nature of the $\mathrm{NO_3^-}$ ion. For the binuclear complex $[\mathrm{Co_2L^2(NO_3)(H_2O)_6}]$, $\nu_3\mathrm{NO_3}$ at 1380 cm^{-1} is split into two vibrations at 1440 and 1325 cm^{-1}, respectively, supporting the coordinated nature of the $\mathrm{NO_3^-}$ ion. For the Co(II) complex of L^4 peaks at 1408, 1330 and 825 cm^{-1} are due to the $\mathrm{NO_2}$ group coordinated to the metal ion. (10) In the Cu^{2+} complexes of all ligands, ν_3S–O is situated at 1150–1160 cm^{-1} supporting the non-coordinated nature of the $\mathrm{SO_4^{-2}}$ ion [15].

The electronic reflectance spectra of the Mn(II) complexes of the ligands under investigation exhibit five bands with $\lambda_{\max}$ situated at 221–290, 329.5–369, 388.5–491, 603–688 and 700–830 nm (Table IV). The first three bands can be assigned to π–π^* transitions within the organic molecule, with those for the C=O and C=N groups being shifted in comparison to the free ligands as a result of complex formation. The last two bands can be assigned to $^6\mathrm{A_{1g}} \rightarrow {}^4\mathrm{T_{2g}}(\mathrm{G})$ and $^6\mathrm{A_{1g}} \rightarrow {}^4\mathrm{T_{1g}}(\mathrm{G})$ transitions, respectively, which may indicate octahedral geometry around the Mn(II) ion [16]. The shift of positions of the bands of complexes compared to those of the ligand to lower or higher wavelengths indicate a formation of six coordinated species [17].

The electronic reflectance spectra of the Co(II) complexes of the ligands also exhibit five bands with $\lambda_{\max}$ situated at 279–287, 337–393, 422–509, 550–692 and 711–850 nm (Table IV). The first three bands can be assigned to π–π^* transitions of C=O, C=N and a ligand to metal charge transfer band (L → Co), respectively, the bands display small shifts from those of the free ligands as a result of complex formation. The last two bands can be assigned to $^4\mathrm{T_{1g}}(\mathrm{F}) \rightarrow {}^4\mathrm{T_{1g}}(\mathrm{P})$ and $^4\mathrm{T_{1g}}(\mathrm{F}) \rightarrow {}^4\mathrm{A_{2g}}$ transitions, respectively, indicating octahedral geometry [18].

The electronic reflectance spectra of the Ni(II) complexes of the ligands exhibit five bands with $\lambda_{\max}$ situated at (274.5–294), (360–397), (447–550), (616–683) and (700–880) nm (Table IV). The first three bands assigned to π–π^* transitions of the C=O, C=N groups and a charge transfer band (L→Ni), respectively, as a result of complex formation. The last two bands can be assigned to $^3\mathrm{A_{2g}} \rightarrow {}^3\mathrm{T_{1g}}(\mathrm{P})$ and $^3\mathrm{A_{2g}} \rightarrow {}^3\mathrm{T_{1g}}(\mathrm{F})$ transitions, respectively, for octahedral geometry around the Ni(II) ion [8].

The electronic reflectance spectra of the Cu(II) complexes of the ligands except for complex of ligand L^2 show mainly five bands with $\lambda_{\max}$ (238.5–292.5), (300–390), (405.5–590), (651.5–750) and (800–860) nm (Table IV). The first three bands can be assigned to π–π^* transitions within the C=O, C=N and a charge transfer band (L→Cu), respectively, the bands display small shifts from those of the free ligands as a result of complex formation. The last two bands can be assigned to the electronic transitions $^2\mathrm{B_{1g}} \rightarrow {}^2\mathrm{B_{2g}}$ and $^2\mathrm{E_g} \rightarrow {}^2\mathrm{T_{2g}}$ which are relevant to an octahedral arrangement of the ligands around the central Cu(II) ion. The Cu(II) complex of the ligand L^2, also shows five bands with $\lambda_{\max}$ at 254.5, 320, 408.5, 730 and 800 nm. The first

TABLE IV Visible spectra and magnetic moment values of Mn(II), Co(II), Ni(II) and Cu(II) complexes of semicarbazone in nujol mull

Complex	*Color*	λ_{max} (nm)				λ_{max} (nm)	*Assignment*	*Magnetic moment* (B.M)
		*π–π** *aromatic ring*	*π–π** *C=O*	*π–π** *C=N*	*C. T* *L → Co* *L → Ni* *L → Cu*			
$[Mn\ L^1(H_2O)_3]Cl \cdot 3H_2O$	Gray	244	330	388.5	–	625.4 733	$^6A_{1g} \rightarrow {}^4T_{2g}(G)$ $^6A_{1g} \rightarrow {}^4T_{1g}(G)$	5.81
$[Mn_2\ L^2Cl_2(H_2O)_5] \cdot 6H_2O$	Gray	244	338	404	–	632 710	$^6A_{1g} \rightarrow {}^4T_{2g}(G)$ $^6A_{1g} \rightarrow {}^4T_{1g}(G)$	4.05
$[MnL^3(H_2O)_3]Cl \cdot H_2O$	Brown	275	360	410	–	606 708	$^6A_{1g} \rightarrow {}^4T_{2g}(G)$ $^6A_{1g} \rightarrow {}^4T_{1g}(G)$	6.1
$[MnL^4(H_2O)_3Cl_2 \cdot 3H_2O$	Dark brown	266	338	446	–	638 700	$^6A_{1g} \rightarrow {}^4T_{2g}(G)$ $^6A_{1g} \rightarrow {}^4T_{1g}(G)$	5.03
$[CoL^1(H_2O)_3]NO_3 \cdot 5H_2O$	Brown	–	282	343	452	625 750	$^4T_{1g}(F) \rightarrow {}^4T_{1g}(P)$ $^4T_{1g}(F) \rightarrow {}^4A_{2g}$	4.48
$[Co_2L^2(NO_3)(H_2O)_6]$	Olive green	–	279	–	422	550 711	$^4T_{1g}(F) \rightarrow {}^4T_{1g}(P)$ $^4T_{1g}(F) \rightarrow {}^4A_{2g}$	3.84
$[CoL^3(H_2O)_3]NO_3 \cdot EtOH$	Olive green	–	287	372	492	692 850	$^4T_{1g}(F) \rightarrow {}^4T_{1g}(P)$ $^4T_{1g}(F) \rightarrow {}^4A_{2g}$	4.93
$[CoL_2{}^4] \cdot 2EtOH$	Brown	–	288	359	500	628 775	$^4T_{1g}(F) \rightarrow {}^4T_{1g}(P)$ $^4T_{1g}(F)^4A_{2g}$	–
$[NiL^1(H_2O)_3]Cl \cdot 2H_2O \cdot EtOH$	Light green	–	277	368	499	646 825	$^3A_{2g} \rightarrow {}^3T_{1g}(P)$ $^3A_{2g} \rightarrow {}^3T_{1g}(F)$	2.74
$[Ni_2L^2(Cl)_2(H_2O)_5]$	Green	–	288	362	500	670 880	$^3A_{2g} \rightarrow {}^3T_{1g}(P)$ $^3A_{2g} \rightarrow {}^3T_{1g}(F)$	1.78
$[NiL^3(H_2O)_5]Cl \cdot 4H_2O$	Green	–	283	360	525	676 870	$^3A_{2g} \rightarrow {}^3T_{1g}(P)$ $^3A_{2g} \rightarrow {}^3T_{1g}(F)$	3.18
$[NiL^4(EtOH)_2\ H_2O]Cl_2 \cdot H_2O$	Green	–	294	365	510	643 809	$^3A_{2g} \rightarrow {}^3T_{1g}(P)$ $^3A_{2g} \rightarrow {}^3T_{1g}(F)$	3.46
$[CuL^1(H_2O)_3]_2SO_4 \cdot 2H_2O \cdot EtOH$	Dark green	–	276	306	421	686 850	$^2E_g \rightarrow {}^2T_{2g}$ $^2B_{1g} \rightarrow {}^2B_{2g}$	1.83
$[Cu_2L^2(H_2O)_3]_2SO_4 \cdot H_2O$	Brown	–	254.5	320	408.5	730 800	$^2B_{1g} \rightarrow {}^2E_g$ $^2B_{1g} \rightarrow {}^2B_{2g}$	1.44
$[CuL^3(H_2O)_2(EtOH)_2SO_4$	Dark brown	–	238.5	313	412	704 880	$^2E_g \rightarrow {}^2T_{2g}$ $^2B_{1g} \rightarrow {}^2B_{2g}$	1.61
$[CuL^4(H_2O)_3]SO_4 \cdot 2H_2O$	Dark brown	–	265.5	300	405.5	651.5 825	$^2E_g \rightarrow {}^2T_{2g}$ $^2B_{1g} \rightarrow {}^2B_{2g}$	2.2

three bands can be assigned to π–π^* transitions within the C=O, C=N and a charge transfer band (L→Cu), respectively. The last two bands can be assigned to $^2B_{1g} \rightarrow {}^2E_g$ and $^2B_{1g} \rightarrow {}^2B_{2g}$ transitions within the energy level diagram of Cu^{2+} by considering a highly distorted octahedral arrangement through tetragonal elongation leading finally to the square planar geometry. This is due to the strong splitting of Jahn–Teller unstable octahedral ground state term $^2B_{1g}$. However, it was suggested that highly split $^2B_{1g}$ ground state and consequently an overlapping with the splitting term ^2E_g lead to a spectral pattern that is characteristic of a square planar geometry [19]. It is interesting to mention that Cu(II) complexes possess two symmetries, octahedral geometry around Cu(II) ion for 1 : 1 (M : L) complexes and square planar for 2 : 1 (M : L) complexes.

Magnetic Properties

The values of the magnetic moments of Mn(II), Co(II), Ni(II) and Cu(II) mononuclear complexes of L^1, L^3 and L^4 with d^5, d^7, d^8 and d^9 ions lie within the range (5.03–6.1), (4.48–4.93), (2.74–3.46) and (1.6–2.2) BM, respectively (Table V). The magnetic moment values of Mn(II), Co(II) and Cu(II) binuclear complexes of L^2 ligand with d^5, d^7, d^8 and d^9 ions amounted to 4.05, 3.86, 1.78 and 1.44 BM, respectively. These values are lower than the proper spin only values, due to the presence of the two adjacent metal ions in the binuclear complexes and subsequent antiferromagnetic exchange [8].

Antimicrobial Screening

Agar disc diffusion was used to test for antimicrobial activity. Assay of the compounds follows.

TABLE V Antimicrobial activity of the semicarbzones and their complexes

Compound	*Clear zone* (cm) *nujol mull*	*% Inhibition*
L^1	2.55	28.33
L^1Mn	2.77	30.86
L^1Co	5.33	59.25
L^1Ni	5.89	65.44
L^1Cu	4.55	50.61
L^2	5.11	56.77
L^2Mn	5.55	61.73
L^2Co	2.56	28.30
L^2Ni	4.22	46.90
L^2Cu	2.88	32.00
L^3	4.33	48.15
L^3Mn	4.55	50.62
L^3Co	4.56	50.00
L^3Ni	4.77	53.08
L^3Cu	6.00	66.66
L^4	1.33	14.81
L^4Mn	1.60	17.78
L^4Co	2.00	22.22
L^4Ni	3.00	33.33
L^4Cu	3.44	38.27

Filter paper discs impregnated with each of the investigated compounds as a nujol mull was placed on the surface of Czapeck's agar medium seeded with *Alternaria alternata* at 30°C and incubated for seven days, then the average diameter of the inhibition zone was recorded for each compound. The results are shown in Table V. All the complexes and ligands were found to be highly active against the fungus. The metal complexes were found to be more active in all cases than their corresponding ligands (Table V), confirming that chelation of metal to ligand increases the toxicity of the compound [3].

The growth inhibition capacity of all complexes of L^1 follows the order $Ni^{II} > Co^{II} > Cu^{II} > Mn^{II}$, also the growth inhibition capacity of all complexes of L^3 and L^4 follows the order $Cu^{II} > Ni^{II} > Co^{II} > Mn^{II}$ but L^2 complexes show different behavior in Table V.

CONCLUSION

Based on the above results, the structure of the complexes under investigation can be formulated as follows (Figs. 1–6):

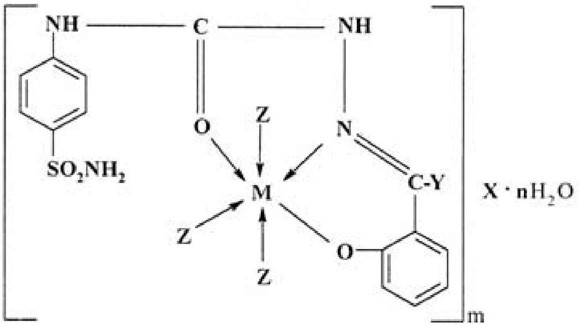

FIGURE 1 Octahedral structures of metal complexes of ligands L^1 and L^3; Y=H and CH_3, respectively; Z = a solvent molecule, H_2O and/or EtOH; X = Cl^-, NO_3^- or SO_4^{2-}; M=Mn(II), Co(II), Ni(II) or Cu(II); m = 1 (X = Cl^-, or NO_3^-); 2 (X = SO_4^{2-}) for values of n see Table I.

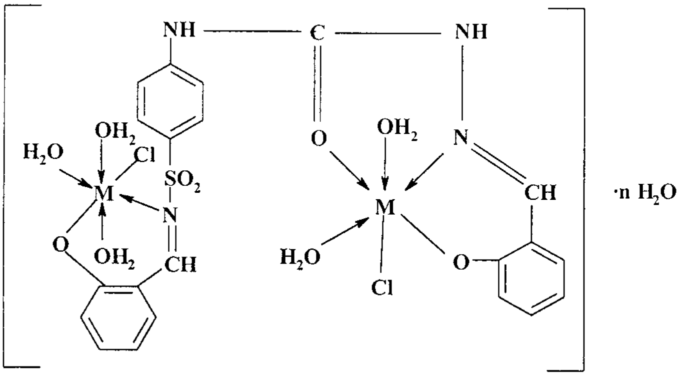

FIGURE 2 Octahedral structures of metal complexes of ligand L^2, M=Mn(II) or Ni(II).

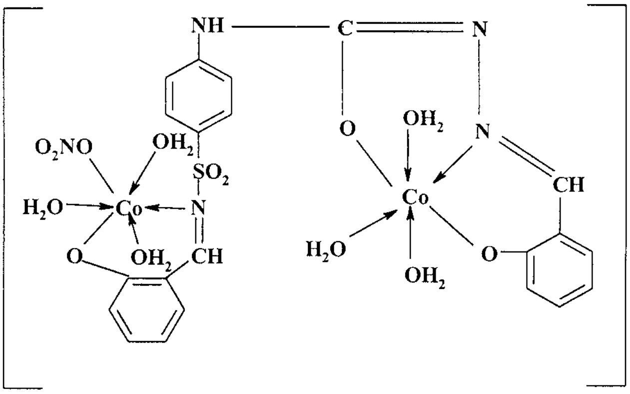

FIGURE 3 Octahedral structures of Co(II) complex of ligand L^2.

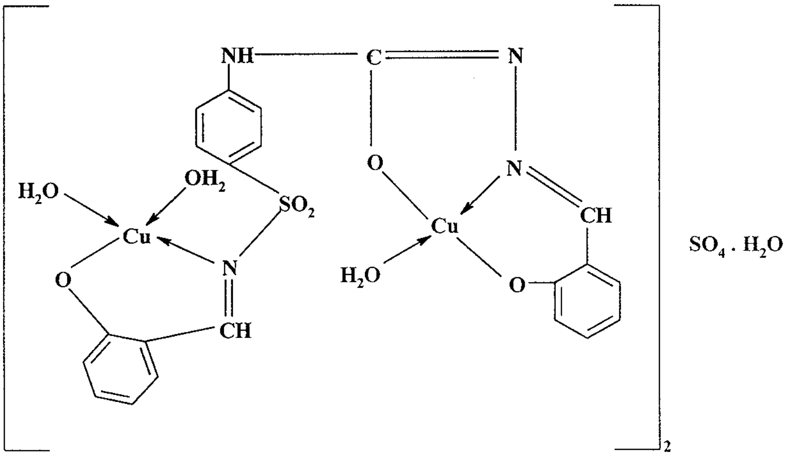

FIGURE 4 Square planar structure of Cu(II) complex of ligand L^2.

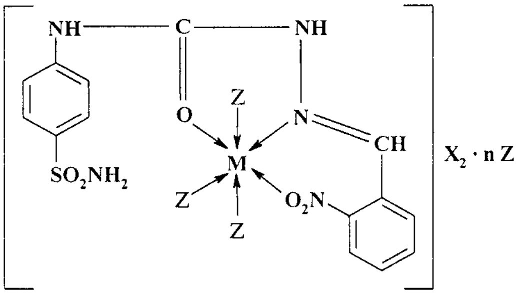

FIGURE 5 Octahedral structures of metal complexes of ligand L^4 M=Mn(II), Ni(II) or Cu(II); $X_2 = 2Cl^-$ or SO_4^{2-}; Z=EtOH and/or H_2O.

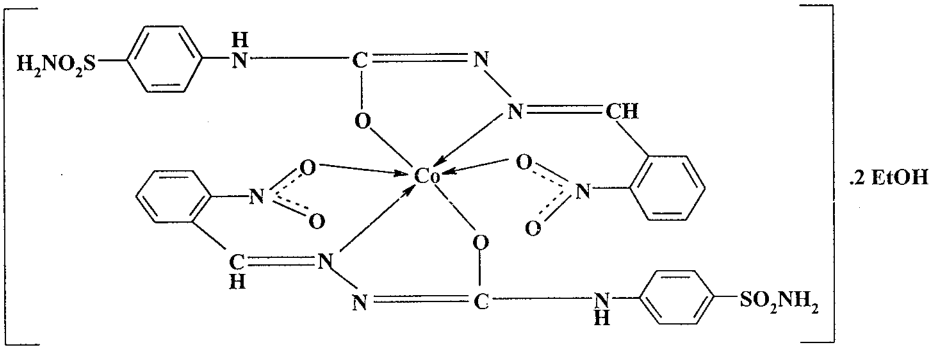

FIGURE 6 Octahedral structures of Co(II) complex of ligand L^4.

References

[1] Y.D. Kulkarni and A. Rowhani, *J. Indian Chem. Soc.* **67**, 46 (1990).

[2] D.X. West, A.E. Liberta, S.B. Padhye, P.B. Chikate, A.S. Sonawane, O. Kumbhar and R.G. Yerande, *Coord. Chem. Rev.* **49**, 123 (1993).

[3] A. Singh, Lalita, R. Dhakarey and G.C. Saxena, *J. Indian Chem. Soc.* **73**, 339 (1996).

[4] F. Hueso, Urêna, A.L. Penâs. Chamarro, M.N. Moreno Carretero, M. Quirós Obozábal and J.M. Salas. Peregrin, *polyhedron* **18**, 351 (1999).

[5] J. Eugeñio, J.C. Graúdo, N.L. Speziali, A. Abras, M. Hörner and C.A.L. Filgueiras, *Polyhedron* **18**, 2483 (1999).

[6] A.A. Saleh and R.J. Crutchley, *J. Inorg. Chem.* **29**, 2132 (1990).

[7] S.M.E. Khalil, *J. Coord. Chem.* **52**, 73 (2000).

[8] T.M.A. Ismail and A.A. Saleh, *Egypt. J. Chem.* **43**(3), 227 (2000).

[9] A. Saxena, J.K. Koacher and J.P. Tandon, *J. Inorg. Nucl. Chem.* **43**(12), 3091 (1981).

[10] S. Satapathy and B. Sahoo, *J. Inorg. Nucl. Chem.* **32**, 2223 (1970).

[11] G.M.H. Sonar, A.S.R. Murty and G.L. Tembe, *J. Indian Chem. Soc.* **72**, 677 (1995).

[12] R. Dhakarey and G.C. Saxena, *J. Chin. Chem. Soc.* **32**, 35 (1985).

[13] C.P. Probhakaran, M.L. Hariku and M. Nair, *J. Indian Chem. Soc.* **75**, 7 (1998).

[14] N.S. Biradar and V.H. Kulkarni, *J. Inorg. Nucl. Chem.* **33**, 2451 (1971).

[15] K. Nakamoto, *Infrared and Raman Spectra of Inorganic and Coordination Compounds*, 4th Edn. (Wiley, Interscience, New York, 1980) p. 258.

[16] F.A. Cotton, D.M.I. Gave and A. Sacce, *J. Am. Chem. Soc.* **83**, 4175 (1961).

[17] A.B.P. Lever, *Inorganic Electronic Spectroscopy* (Elsevier, Amsterdam, 1968).

[18] K.C. Satpathy, R. Mishra and B.B. Jal, *J. Indian Chem. Soc.* **68**, 377 (1986).

[19] B.S. Hathaway and D.E. Billing, *Coord. Chem. Rev.* **5**, 143 (1970).